Check for updates

Geophysical Research Letters

RESEARCH LETTER
10.1029/2026GL124079

Quantifying Deep Ocean Methane Along the Central Chilean Margin

Scott T. Wieman[1,2], Adam Skarke[3], Jeff Beeson[4,5], Erin Frates[6], Lucía Villar-Muñoz[7], Davide Oppo[8], Sarah Youngs[9], Jason Kapit[9], Eulogio Soto[10], Jeffrey J. Marlow[6], and Anna P. M. Michel[9]

[1]The MIT-WHOI Joint Program in Oceanography/Applied Ocean Science and Engineering, Woods Hole, MA, USA, [2]Department of Geology and Geophysics, Woods Hole Oceanographic Institution, Woods Hole, MA, USA, [3]Department of Geosciences, Mississippi State University, Mississippi State, MS, USA, [4]College of Earth, Ocean, and Atmospheric Sciences, Oregon State University, Corvallis, OR, USA, [5]Pacific Marine Environmental Laboratory, National Oceanic and Atmospheric Administration, Newport, OR, USA, [6]Department of Biology, Boston University, Boston, MA, USA, [7]Departamento de Geofísica, Facultad de Ciencias Físicas y Matemáticas, Universidad de Chile, Santiago, Chile, [8]Department of Oceanography, Texas A&M University, College Station, TX, USA, [9]Department of Applied Ocean Physics and Engineering, Woods Hole Oceanographic Institution, Woods Hole, MA, USA, [10]Centro de Observación y Análisis del Océano Costero, Facultad de Ciencias del Mar y de Recursos Naturales, Universidad de Valparaíso, Valparaíso, Chile

Key Points:

- 68 gas flares were discovered along the central Chilean Margin, 59 of which were within three known or suspected seep areas
- We estimate 69.2 tons of gaseous methane is emitted annually from the sediments to the seawater at the three seepage areas
- We estimate the presence of 1.9 tons of dissolved methane in near-seafloor waters as a result of gas flares across the three seepage areas

Supporting Information:

Supporting Information may be found in the online version of this article.

Correspondence to:

S. T. Wieman and A. P. M. Michel,
scott.wieman@whoi.edu;
amichel@whoi.edu

Citation:

Wieman, S. T., Skarke, A., Beeson, J., Frates, E., Villar-Muñoz, L., Oppo, D., et al. (2026). Quantifying deep ocean methane along the central Chilean Margin. *Geophysical Research Letters*, *53*, e2026GL124079. https://doi.org/10.1029/2026GL124079

Received 30 APR 2026
Accepted 24 SEP 2026

Author Contributions:

Conceptualization: Scott T. Wieman, Adam Skarke, Anna P. M. Michel
Data curation: Adam Skarke, Jeff Beeson
Formal analysis: Scott T. Wieman, Adam Skarke, Jeff Beeson
Funding acquisition: Eulogio Soto, Jeffrey J. Marlow, Anna P. M. Michel
Investigation: Scott T. Wieman, Adam Skarke, Jeff Beeson, Erin Frates, Lucía Villar-Muñoz, Davide Oppo
Methodology: Scott T. Wieman, Adam Skarke, Jeff Beeson

© 2026 The Author(s). Geophysical Research Letters published by Wiley Periodicals LLC on behalf of American Geophysical Union.
This is an open access article under the terms of the Creative Commons Attribution-NonCommercial License, which permits use, distribution and reproduction in any medium, provided the original work is properly cited and is not used for commercial purposes.

Abstract Cold seeps are dynamic seafloor environments that provide conduits for methane (CH_4) to be transferred from marine sediments to the global ocean and, in shallow settings, the atmosphere. These seeps are ubiquitous along continental margins yet their spatial extent and impact on the marine carbon cycle are poorly constrained. During a research expedition to the underexplored Chilean Margin, we utilized an ROV-mounted in situ CH_4 sensor and multibeam sonar to map seep fields. We confirmed seepage at depths between 100 and 2,750 m at El Quisco Seep Site, Concepción Methane Seep Area, and Mocha Island Seep Area. Combining ship-based and ROV-based acoustic gas flare detection with real-time dissolved CH_4 measurements three different manifestations of CH_4 seepage were identified, which enabled estimations of both sediment-seawater gaseous CH_4 flux (69.2 ± 11.2 t/yr) and near-seafloor dissolved CH_4 storage (1.9 ± 1.3 t) along the central Chilean Margin.

Plain Language Summary Marine sediments host the largest amount of methane on the planet, but across most of the seafloor it is wholly consumed by microbes. However, at some places rapid fluid flow transports methane through the sediments and into the ocean. These locations, called cold seeps, are found on continental margins around the globe, and their distribution and role in the marine carbon cycle is widely studied across the Northern Hemisphere. The Southern Hemisphere is less studied, leading to a paucity of our understanding of seeps there. We present here the results of an expedition along the central Chilean Margin where we confirmed the presence of methane seepage, discovered new seeps, and quantified both the gaseous methane efflux from the sediments into the seawater as well as the total amount of dissolved methane in near-seafloor waters through coupled dissolved gas measurements and acoustic bubble detection.

1. Introduction

Methane (CH_4) is a potent greenhouse gas, and marine sediments contain the largest reservoir of CH_4 on Earth's surface (Ruppel & Kessler, 2017; Weber et al., 2019). Sedimentary CH_4 is primarily stored in vast volumes of ice-like gas hydrates, which are metastable structures that are thought to host ~500 GtC of methane globally (Piñero et al., 2013; Wallmann et al., 2012). In most settings, CH_4 migrating up through the sediments is fully consumed by anaerobic oxidation, which is carried out by methanotrophic archaea and sulfate-reducing bacteria (Knittel & Boetius, 2009; J. J. Marlow et al., 2014; Reeburgh, 2007). However, in some places the upward CH_4 flux in shallow sediments is particularly high and its transportation is aided by structural migration pathways such as faults, which enable large quantities of CH_4 to reach the sediment-seawater interface at sites termed cold seeps (Suess, 2010). While cold seeps only cover a small fraction of the seafloor, they are dynamic environments that form biodiverse oases of endemic chemosynthetic life in the deep sea (Åström et al., 2018; German et al., 2011). Many seeps also overlay gas hydrates (Suess, 2010) which can be quickly destabilized through rapid changes in pressure and temperature, such as slope failure, seismic activity, or local warming (Ezat et al., 2014). The release of large quantities of methane from hydrates has been proposed as a potential cause of past major climatic changes

19448007, 2026, 20, Downloaded from https://agupubs.onlinelibrary.wiley.com/doi/10.1029/2026GL124079 by Cochrane Chile, Wiley Online Library on [12/10/2026]. See the Terms and Conditions (https://onlinelibrary.wiley.com/terms-and-conditions) on Wiley Online Library for rules of use; OA articles are governed by the applicable Creative Commons License

Project administration: Eulogio Soto, Jeffrey J. Marlow
Resources: Sarah Youngs, Jason Kapit, Eulogio Soto, Anna P. M. Michel
Software: Sarah Youngs, Jason Kapit, Eulogio Soto
Supervision: Anna P. M. Michel
Visualization: Scott T. Wieman, Adam Skarke, Jeff Beeson
Writing – original draft: Scott T. Wieman
Writing – review & editing: Scott T. Wieman, Adam Skarke, Jeff Beeson, Erin Frates, Lucía Villar-Muñoz, Davide Oppo, Eulogio Soto, Jeffrey J. Marlow, Anna P. M. Michel

(Weldeab et al., 2022), and the response of current hydrate reserves to ongoing and future environmental changes is uncertain (Kennett et al., 2000).

The discovery, mapping, and cataloging of global hydrates, cold seeps, and marine methane fluxes is an ongoing effort across governmental, non-governmental, and academic institutions. Cold seeps are most often found along active and passive continental margins (Suess, 2010). Some areas of seepage are extensively studied, such as the Cascadia Margin (Boetius & Suess, 2004; Luff & Wallmann, 2003; Suess, 2014) and the Norwegian Continental Shelf (Argentino et al., 2022; Panieri et al., 2017; Yao et al., 2021), but other regions, particularly in the Southern Hemisphere, remain frontiers for exploration and discovery.

The Chilean Margin is one of the longest convergent margins, and rapid subduction drives significant uplift resulting in extensive erosion and high supply of organic-rich terrigenous material to marine environments (Carretier et al., 2018; Garreaud, 2009; Lamy et al., 1998). Methane seepage along the central Chilean Margin has traditionally been interpreted as predominantly biogenic, largely linked to high organic carbon supply and enhanced methanogenesis under oxygen minimum zone conditions (Muñoz et al., 2023). However, CH_4 seepage in highly tectonically active regions of the Chilean Margin, such as Mocha Island, may also be strongly influenced by fault-controlled fluid migration within the accretionary prism, transporting deeper sourced free gas and methane enriched fluids along the sedimentary column (Vargas-Cordero et al., 2017, 2018, 2021). While the full margin has not been systematically mapped, seepage has been proposed at four distinct sites along the central Chilean Margin (i.e., Limarí, El Quisco Seep Site (EQSS), Concepción Methane Seep Area (CMSA), and Mocha Island Seep Area (MISA)) based on indirect evidence such as the recovery of chemosynthetic organisms (Melo et al., 2007; Muñoz et al., 2016; Sellanes et al., 2004, 2008), trophic ecology studies (Zapata-Hernández et al., 2014), and documentation of gas flares (Klaucke et al., 2012; Vargas-Cordero et al., 2018).

In October–November 2024, a research expedition aboard the *R/V Falkor(too)* (Fkt241011) sailed from Valparaíso to Puerto Montt (Chile) to locate, characterize, and sample CH_4 seeps at all four proposed seepage areas (Figure 1a) along the central Chilean Margin. We present here mapped gas flares, fingerprints of methane seepage, estimates of the gaseous CH_4 flux to the seawater, and calculations of near-seafloor dissolved CH_4 at the El Quisco, Concepción, and MISAs.

2. Materials and Methods

Potential seep areas were broadly surveyed using ship-mounted multibeam echosounder (MBES; EM124 and EM712, Kongsberg, Norway). MBES data were used to identify gas flares in the water column, generate bathymetric maps, and identify seafloor areas exhibiting enhanced consolidation such as carbonate concretions, tubeworm mounds, and clam beds. These three factors were used to define regions of interest for ROV *SuBastian* dives. ROV *SuBastian* was outfitted with a dissolved CH_4 sensor (Sensor for Aqueous Gases in the Environment (SAGE) (Kapit & Michel, 2021; Kapit et al., 2024), Woods Hole Oceanographic Institution, USA), a downward-facing multibeam sonar (M3, Kongsberg, Norway) for mapping, a CTD (FastCAT SBE49, Sea-Bird Scientific, USA) for temperature and salinity measurements, and a dissolved oxygen (DO) sensor (3841 oxygen optode, Aanderaa, Norway). The real-time readout of ROV-based multibeam coupled with dissolved CH_4 data enabled rapid identification of target locations for subsequent seafloor exploration.

2.1. Ship-Based Mapping

Ship-based seafloor mapping was conducted with a 40–100 kHz multibeam sonar (EM712) for shallower water depths (~100–1,200 m) and a 10.5–13.5 kHz multibeam sonar (EM124) for deeper water depths (~500–4,800 m), depending on the surveyed location. Dedicated multibeam site surveys were designed with a swath overlap of >50% to ensure robust seafloor coverage. Resulting raw seafloor sounding data were processed to correct for sound speed and vessel motion and manually filtered to remove noise. These data were then gridded at a resolution commensurate with water depth at each site (10–50 m^2) to create bathymetric surfaces (Figures 1b–1d).

Water column acoustic backscatter data generated by both multibeam sonar systems were manually reviewed on a ping-by-ping basis in fanbeam as well as along-track profiles for the presence of water column features consistent with gas flares generated by CH_4 seeps. These features generally appeared as linear to sub-linear vertical volumes of elevated acoustic reflectivity due to the substantial impedance contrast between free gas and water. Identified gas flares were traced to their point of intersection with the seafloor to establish the location of CH_4 seeps.

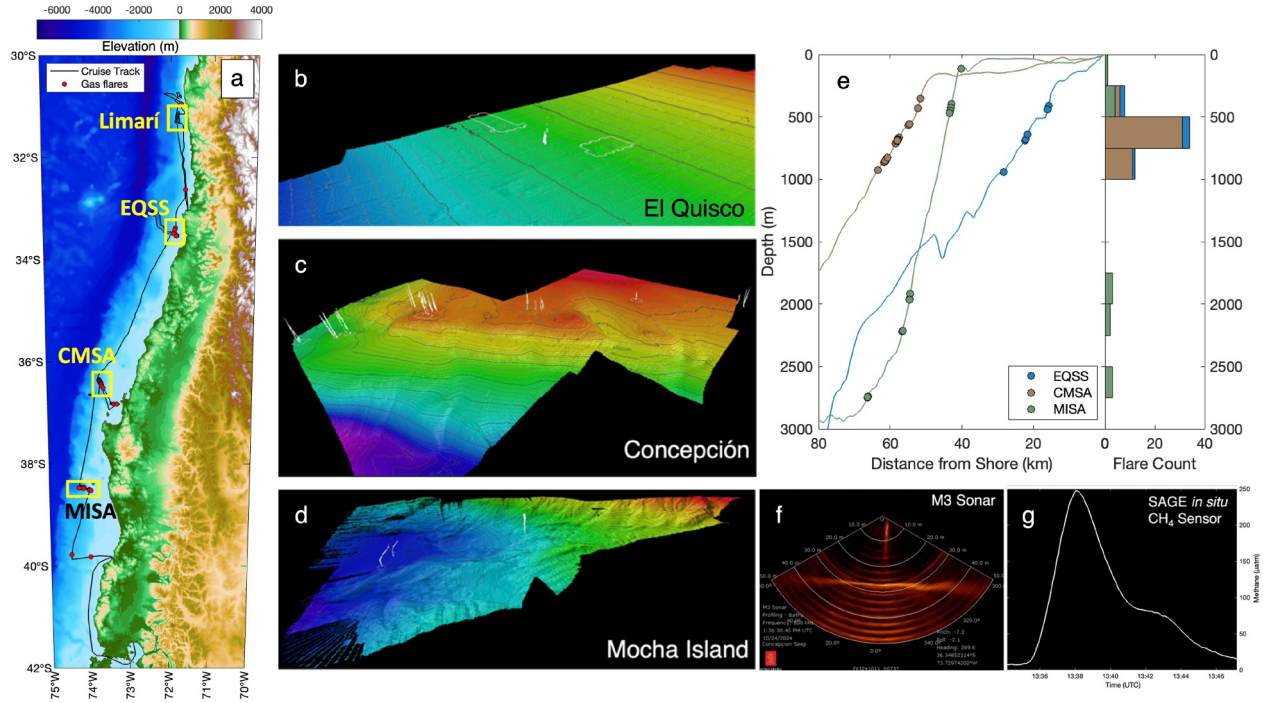


Figure 1. Map (a) of the cruise track of FKt241011 along the central Chilean Margin including flares (red dots) and seep sites (yellow outlines). Bathymetry (b–d) of confirmed seepage areas showing identified gas flares in each region. The distribution (e) of gas flares with depth at the three confirmed seepage areas shows most originate above 1,000 m though there are several deeper flares at MISA. Flare positions are plotted against average longitudinal bathymetric profiles for each seepage area. Near-seafloor observations to identify local seepage included (f) acoustic detection of gas flares and (g) real-time measurement of CH_4 partial pressure using a SAGE (Sensor for Aqueous Gases in the Environment) instrument.

2.2. ROV-Based Mapping

During dives, ROV *SuBastian* was flown at 20–30 m above the seafloor in a grid pattern to map regions of interest (Figure S1 in Supporting Information S1). Vehicle control was based on terrain: the ROV maintained auto-altitude where bottom relief was moderate and used auto-depth or manual piloting where bottom relief was highly variable to ensure a safe height off bottom and maintain consistent coverage/overlap. ROV attitude (pitch, yaw, and roll) and position (latitude, longitude, and depth) were provided by the SPRINT-Nav hybrid navigation system (Sonardyne, UK). The M3 sonar was operated at ∼700 kHz with a variable ping rate. Navigation and attitude messages were logged at 1 Hz and applied within the processing workflow for georeferencing and motion compensation. Sound-speed information used for refraction correction was derived from the onboard CTD.

Raw ROV multibeam data were recorded in native .mmb/.imb formats and converted to Kongsberg.all format for downstream processing and compatibility with standard swath-processing tools. Bathymetric processing and ping-level editing were performed using MB-System. Processing steps included: (a) merging and time-aligning asynchronous time series data to the converted sonar files with the 1 Hz SPRINT-Nav navigation/attitude stream; (b) applying CTD-derived sound-speed information for refraction correction; and (c) interactive ping editing to remove outliers and artifacts (e.g., edge-of-swath artifacts, intermittent dropouts). Cleaned soundings were gridded to generate high-resolution bathymetric surfaces, typically at 1 m^2 cell size.

2.3. Dissolved CH_4 Sensing

SAGE is a compact gas sensor capable of measuring dissolved CH_4 in the ocean (Kapit et al., 2024; Kapit & Michel, 2021). It utilizes a gas-permeable, water-impermeable membrane to extract gases from seawater, which are then passed through a 5m-long hollow core fiber (HCF). The gas contained in the HCF is continuously irradiated by a near-infrared tunable diode laser being scanned across the spectral region of interest. Absorption spectra are collected at a sampling rate of 1 Hz and converted to the partial pressure of CH_4 (pCH_4) in the fiber. pCH_4 is converted to nanomoles of CH_4 following Wiesenburg and Guinasso (1979). SAGE has been previously

19448007, 2026, 20, Downloaded from https://agupubs.onlinelibrary.wiley.com/doi/10.1029/2026GL124079 by Cochrane Chile, Wiley Online Library on [12/10/2026]. See the Terms and Conditions (https://onlinelibrary.wiley.com/terms-and-conditions) on Wiley Online Library for rules of use; OA articles are governed by the applicable Creative Commons License

deployed at hydrothermal vents (Kapit et al., 2024; Preston et al., 2022) and CH_4 seeps (Padilla et al., 2025) to map concentrations of dissolved CH_4.

To correct for the residence time of gas in the HCF, each CH_4 time series was deconvoluted to instantaneous water column measurements using the MATLAB Lucy deconvolution function DECONVLUCY with five iterations and a damping threshold of 1. The point spread function was derived from fitting an exponentially modified Gaussian to a best-estimate single impulse response observed during Dive SO744 at MISA.

2.4. Flux and Near-Seafloor Storage Estimation

Gas-phase CH_4 fluxes across the sediment-seawater interface were estimated through seafloor bubble counting and seafloor conditions. Bubbles were manually counted for at least one continuous minute from video footage at times when the ROV remained stationary. Estimated rates were calculated for each gas flare based on the average bubble diameter documented at seep sites globally (4.65 ± 1.47 mm, Table S1 in Supporting Information S1), the number of bubble plumes per gas flare based on seafloor observations (3.2 ± 1.9), the average bubble emission rate (2.9 ± 1.9 bubbles per second), and the water depth of each flare (Table S2 in Supporting Information S1) from which we calculated seafloor temperature (Locarnini et al., 2024) and pressure. While the time intervals used for bubble counting were short, the bubble emission rates for seeps are similar to longer-term observational studies from the South China Sea and Gulf of Mexico (Di et al., 2020; Wang et al., 2016; Wang & Socolofsky, 2015). Gas emissions from seeps are highly variable in time (Greinert, 2008; Marcon et al., 2021), but even with our short observation periods we caught several bursts of bubbles and periods of quiescence. While this data represents a first estimate of gaseous CH_4 fluxes, longer-term studies at seeps along the Chilean Margin are necessary to robustly quantify this flux.

Along-track dissolved CH_4 measurements were converted into spatial maps using the GRIDDATA function in MATLAB with linear interpolation (Figure 2). CH_4 plumes were defined as continuous areas with concentrations exceeding 15 nM (~2σ above water column background). The vertical extent of an average plume was estimated from a profile during Dive SO747 at MISA, which captured the upper half of a CH_4 plume. This plume was well-described by a Gaussian with a c of 5.7 m ($r^2 = 0.97$). Dissolved CH_4 for the near-seafloor water column was calculated by multiplying the interpolated CH_4 concentration by the x-y resolution of the interpolation (0.25 m^2) and the integrated area under the normalized Gaussian describing the plume (14.29 m). The total near-seafloor dissolved CH_4 was calculated by averaging together the dissolved CH_4 associated with each gas flare and scaling up to the number of observed gas flares at each seep site. Without multiple observations in time, we necessarily assume that the observed amount and distribution of dissolved CH_4 represents its steady state storage in near-seafloor waters.

3. Results and Discussion

3.1. Complementary Value of Acoustic and In Situ Measurements

Our work extends the evidence for CH_4 seepage on the Chilean Margin through multibeam imaging of 68 gas flares (Table S2 in Supporting Information S1) along the cruise track, near-seafloor imaging of gas flares, and measurements of elevated CH_4 concentrations at seven different dive sites (Figure S1, Table S3 in Supporting Information S1). Paired acoustic data and dissolved CH_4 measurements from ROV mapping confirmed active seepage at EQSS, CMSA, and MISA, with no signs of seepage observed at Limarí. Most seepage occurred between 400 and 1,000 m water depth with some gas flares at MISA found at >1,900 m water depth (Figure 1e). Acoustic water-column imaging and in situ CH_4 analysis provided distinct and complementary indicators of seepage. Across sites, we documented CH_4 plumes (continuous regions of elevated dissolved CH_4) and gas flares (bubble streams released directly into the water column). Coupling these two techniques was essential to identify all expressions of seepage, as neither method alone captured all seepage points.

3.2. Differing Manifestations of CH_4 Seepage at Chilean Seeps

By combining ROV-based acoustic gas detection and in situ CH_4 measurements, we were able to identify three different types of CH_4 seepage along the central Chilean Margin: Type 1: coupled gas flares and dissolved CH_4 plumes; Type 2: gas flares without any associated dissolved CH_4 plume; and Type 3: dissolved CH_4 plumes

19448007, 2026, 20, Downloaded from https://agupubs.onlinelibrary.wiley.com/doi/10.1029/2026GL124079 by Cochrane Chile, Wiley Online Library on [12/10/2026]. See the Terms and Conditions (https://onlinelibrary.wiley.com/terms-and-conditions) on Wiley Online Library for rules of use; OA articles are governed by the applicable Creative Commons License

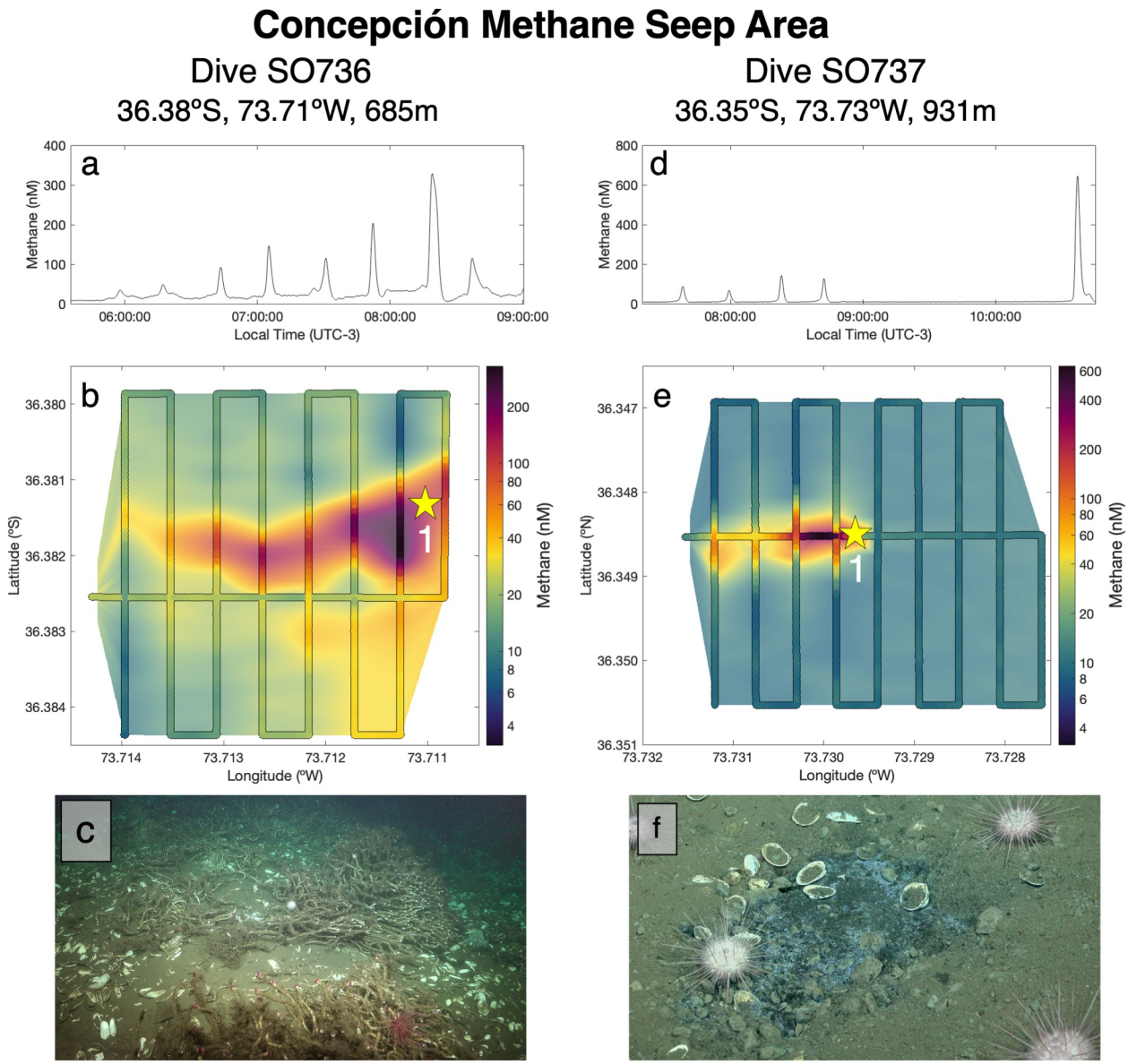


Figure 2. Methane timeseries (a), (d) and interpolated maps of dissolved CH_4 plumes (b), (e) as observed on Dives SO736 (a–c) and SO737 (d–f) at CMSA highlighting observations of Type 1 (see Section 3.2) seepage: co-located gas flares and dissolved CH_4 plumes. Observed gas flares are marked with stars and seafloor observations (c), (f) confirmed bubble emissions and seep fauna at the base of each flare.

without any associated gas flares. We discuss below these three different manifestations and explore the information they can provide about seepage along the Chilean Margin.

1. At many seep sites, strong acoustic returns in near-seafloor multibeam mapping indicated vigorous gas flares that were co-located with plumes of dissolved CH_4 in near-seafloor waters (Figure 2). Based on observations across the four sites where we observe this manifestation of seepage (Table S3 in Supporting Information S1), we calculate that each gas flare produces 10.6 ± 6.8 kg of dissolved CH_4 in near-seafloor waters. We assume this near-seafloor dissolved CH_4 to be representative as we only have a single observation with respect to time for any given gas flare and no water column CH_4 consumption constraints.
2. On Dive SO744 at MISA, we identified a vigorous gas flare via near-seafloor mapping, but this flare was not associated with any increase in dissolved CH_4 (Figure 3b). This lack of dissolved CH_4 coupled with the high pressure (22.4 MPa) and low temperature (1.9°C) suggests hydrated bubbles that prevent CH_4 exchange into the water column. A slow-dissolving hydrated shell is consistent with field experiments (Rehder et al., 2009)

19448007, 2026, 20, Downloaded from https://agupubs.onlinelibrary.wiley.com/doi/10.1029/2026GL124079 by Cochrane Chile, Wiley Online Library on [12/10/2026]. See the Terms and Conditions (https://onlinelibrary.wiley.com/terms-and-conditions) on Wiley Online Library for rules of use; OA articles are governed by the applicable Creative Commons License

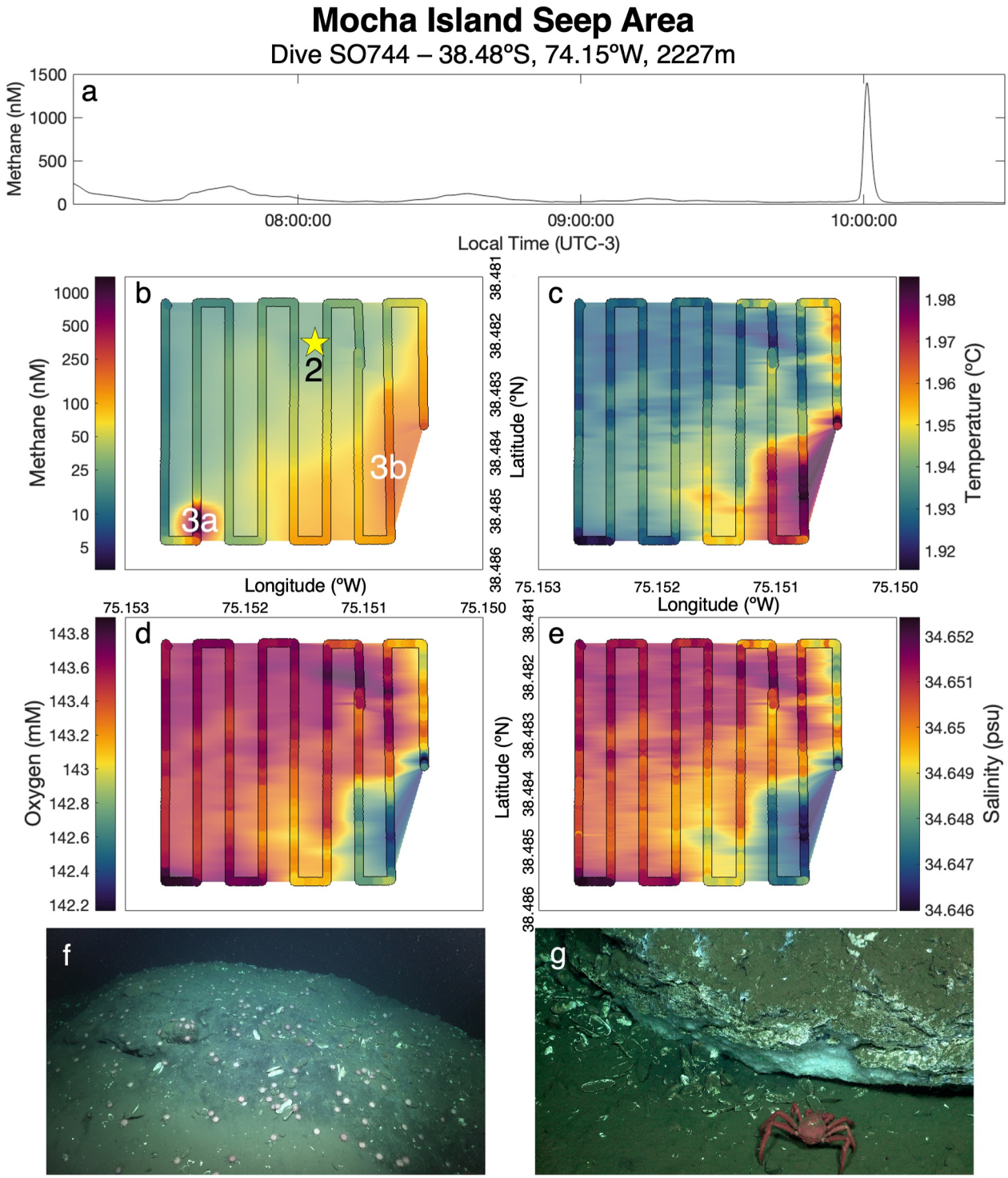


Figure 3. Methane timeseries (a) and interpolated maps of (b–e) dissolved CH_4, dissolved oxygen, water temperature, and salinity as observed on Dive SO744 at MISA. Seafloor observations (f–g) confirmed seep fauna at the location of both (2) the strong gas flare and (3a) the localized CH_4 anomaly. The origin of the diffuse plume (3b) is unknown as seafloor observation did not progress to the source.

showing slower bubble dissolution rates within the gas hydrate stability zone, and seafloor observations confirmed exposed hydrates at the base of this gas flare. While the upper limit of CH_4 hydrate stability along the central Chilean Margin is at ~550 m water depth, we observed extensive dissolved CH_4 associated with gas flares down to depths of ~1,000 m (Figure 2; Table S3 in Supporting Information S1). However, with no gas

19448007, 2026, 20, Downloaded from https://agupubs.onlinelibrary.wiley.com/doi/10.1029/2026GL124079 by Cochrane Chile, Wiley Online Library on [12/10/2026]. See the Terms and Conditions (https://onlinelibrary.wiley.com/terms-and-conditions) on Wiley Online Library for rules of use; OA articles are governed by the applicable Creative Commons License

19448007, 2026, 20, Downloaded from https://agupubs.onlinelibrary.wiley.com/doi/10.1029/2026GL124079 by Cochrane Chile, Wiley Online Library on [12/10/2026]. See the Terms and Conditions (https://onlinelibrary.wiley.com/terms-and-conditions) on Wiley Online Library for rules of use; OA articles are governed by the applicable Creative Commons License

Table 1
Estimates of Dissolved CH_4 Associated With Gas Flares, Number of Gas Flares Detected With Ship-Based Multibeam, and the Upscaled Total Dissolved CH_4 at Each Seepage Area

Location	Number of gas flares	Total dissolved CH_4 (t)	Total gas CH_4 flux (t/yr)	Mapped area (km^2)
EQSS	6	0.22	4.65	19.2
CMSA	42	1.52	37.92	95.8
MISA	13/5[a]	0.18	26.59	331.5
Total	**61/53**[a]	**1.92**	**69.16**	**446.5**

[a]Thirteen gas flares were imaged at MISA, but eight were deeper than 1,000 m and were thus excluded from dissolved CH_4 estimates but included in gaseous CH_4 flux estimates.

flares identified between water depths of ~1,000 m and 1,900 m (Figure 1e; Table S2 in Supporting Information S1) we are unable to pinpoint the transition depth between Type 1 and Type 2 seepage.

3. In addition to the Type 2 seepage at MISA, we observed multiple locations with a third type of seepage, namely dissolved CH_4 plumes without any associated gas flares. On Dive SO744, this seepage took two different forms: a narrow plume in the southwest and a broad diffuse plume across the southeastern portion of the site. The elevated CH_4 plume in the southwestern part of the dive area closely matches seafloor conditions, including highly elevated CH_4 concentrations. This similarity suggests lofting of a seafloor water mass, which could result from either bubble stream entrainment or orographic displacement. While we did not observe bubbles near this plume, bubble releases at seep sites are highly variable in time and may have been missed (Greinert, 2008; Marcon et al., 2021). Seafloor exploration traced this plume to an isolated mound colonized by sea urchins and surrounded by clam beds, and no bubbles were observed.
   The dissolved CH_4 concentration in the broad plume in the southeastern portion of the site was positively correlated with water temperature and negatively correlated with both salinity and DO (Figure S2 in Supporting Information S1), the only plume to show such correlations during the expedition. A decrease in both salinity and DO can be a fingerprint of dissociating hydrates (Elliott et al., 2010; Malinverno et al., 2008), although the relationship between temperature and salinity is consistent with the ROV descent and ascent profiles (Figure S3 in Supporting Information S1). The southeast-northwest trend of the plume aligns with the long-term current direction inferred from bedform morphology (Figure S4 in Supporting Information S1). Although seafloor exploration did not progress far enough to identify the source of this plume, elevated CH_4 was first detected at 2,100 m on the descent and remained elevated all the way to the seafloor (~2,200 m), producing a plume thickness of ~120 m.

3.3. Margin-Wide Estimates of Gaseous CH_4 Flux and Dissolved CH_4 Storage

We estimated the sediment-seawater flux of gas-phase CH_4 by scaling up Type 1 and 2 seepage and estimated the total amount of near-seafloor dissolved CH_4 by scaling up Type 1 seepage. Unfortunately, Type 3 seepage could not be scaled up due to the inability to acoustically detect such seepage from ship-based surveying.

Seafloor observations of individual bubble streams at CMSA (Dive SO737) and MISA (Dives SO744, SO745, SO747) showed release rates of 0.8–7.2 bubbles per second, with a mean release rate of 2.9 ± 1.9 bubbles per second. Using an average bubble diameter of 4.7 ± 1.5 mm (Table S1 in Supporting Information S1), this emission rate is equivalent to 9.1 ± 7.7 mL/min per individual bubble stream, which is comparable to emission rates reported for other individual bubble streams in the literature (Di et al., 2020; Römer et al., 2012, 2014). CH_4 emissions for individual gas flares are calculated using the Redlich-Kwong equation of state with flare-specific pressure and temperature calculated for each flare based on its depth and multiplying by the average number of bubble streams per gas flare observed on dives (3.2 ± 1.9, Table S3 in Supporting Information S1) and the measured average bubble CH_4 composition during the cruise (99.0 ± 0.4%). Based on this calculation, gas flares along the Chilean Margin release 0.24–6.87 mmol CH_4/s, with an average of 2.25 mmol CH_4/s. Nearly all sites are sufficiently deep that this CH_4 does not reach the atmosphere (Joung et al., 2022; Nordam et al., 2025).

Scaling this up based on the number of observed gas flares produces emission estimates of 4.7 ± 2.1 t CH_4/yr (EQSS), 37.9 ± 6.2 t CH_4/yr (CMSA), and 26.6 ± 9.1 t CH_4/yr (MISA) for a total annual CH_4 flux from these three sites of 69.2 ± 11.2 t CH_4/yr (Table 1). Uncertainty bounds represent fully propagated uncertainty in bubble

19448007, 2026, 20, Downloaded from https://agupubs.onlinelibrary.wiley.com/doi/10.1029/2026GL124079 by Cochrane Chile, Wiley Online Library on [12/10/2026]. See the Terms and Conditions (https://onlinelibrary.wiley.com/terms-and-conditions) on Wiley Online Library for rules of use; OA articles are governed by the applicable Creative Commons License

diameter, emission rate, and bubble plumes per flare. The total estimated flux only considers gas flares at the three seep sites, as these locations were the only areas where mapping coverage was high enough to have captured many, if not all, gas flares. Additional flares were identified along the cruise track (Figure 1, Table S1 in Supporting Information S1) and indicate locations where further exploration is warranted.

In addition to gaseous flux calculations, measurements of dissolved CH_4 (Figure 2) coupled with high-accuracy observations of near-seafloor gas flares enable direct calculation of the impact of gas flares on local water chemistry (Table 1). On average, a bubble stream produces 10.6 ± 6.8 kg CH_4 dissolved in near-seafloor waters (Table S3 in Supporting Information S1). Combining these estimates with the number of detected gas flares and estimate of bubble streams per gas flare produces estimates of 0.2 ± 0.2 t (EQSS), 1.5 ± 1.3 t (CMSA), and 0.2 ± 0.2 t (MISA) of dissolved CH_4 for a total of 1.9 ± 1.3 t CH_4 dissolved in near-seafloor waters across these three sites. The estimate of near-seafloor dissolved CH_4 at MISA is based only on gas flares originating above 1,000 m water depth, as a gas flare at ~2,200 m depth during Dive SO744 was not observed to produce elevated CH_4 concentration. This is likely due to bubble coating by hydration shells (Fu et al., 2021), which prevents effective mass transfer between the bubbles and the water column as discussed above.

While the amount of dissolved CH_4 in near-seafloor waters is ~3% of the annual gaseous CH_4 flux out of the sediments, we were unable to measure dissolved fluxes out of the sediments which likely contribute significantly to the total pool of dissolved CH_4 in these near-seafloor waters. Additionally, seep emissions are highly temporally variable, and the half-life for marine biodegradation of dissolved CH_4 is days (Leonte et al., 2018; Nordam et al., 2025) to years (Nordam et al., 2025). Thus, the observed quantity of dissolved CH_4 near the seafloor is likely an integration across significant variations in the sedimentary CH_4 efflux. Given the high concentrations of CH_4 not associated with any gas flares observed during Dive SO744 (Figure 3), this estimate of total dissolved CH_4 is almost certainly a lower bound for the margin.

Near-seafloor dissolved CH_4 plumes associated with gas flares were not associated with any decrease in DO. Across Dives SO730, SO736, and SO737, the difference between DO concentrations within and outside of the CH_4 plume was 0.6 ± 1.6 μM. The CH_4 plume on Dive SO747 had a significantly larger DO concentration difference (36.7 μM higher in the plume), but this site was situated on a steep slope along a large DO gradient that accounts for this variation. The observed lack of effect of CH_4 plumes on DO concentrations in near-seafloor waters agrees with recent observations from seeps on the Hikurangi and US Atlantic Margins (García-Tigreros & Kessler, 2018; Law et al., 2024) and suggests only minor to no impact from aerobic CH_4 oxidation on near-seafloor water column DO budgets along the Chilean Margin.

4. Key Takeaways

Seepage along the Chilean Margin is spatially widespread and exhibits diverse manifestations across and within sites. This work represents the first quantification of the gaseous CH_4 flux along the central Chilean Margin and, to the best of our knowledge, the first estimate of the dissolved near-seafloor CH_4 budget of seeps. We mapped 68 distinct gas flares along the central Chilean Margin, 59 of which were within the EQSS, CMSA, and MISA zones. Near-seafloor acoustic observations and chemical sensing confirmed the presence of extensive cold seep activity via elevated dissolved CH_4 in near-seafloor waters and acoustic detection of near-seafloor gas flares. Seeps were found in water depths of 100–2,750 m, and we identified three different manifestations of CH_4 seepage: co-located gas flares and dissolved CH_4 plumes, gas flares without associated dissolved CH_4, and dissolved CH_4 plumes without associated gas flares. We estimate an annual gaseous CH_4 flux across the sediment-seawater interface of 69.6 ± 11.3 t CH_4/yr and a dissolved CH_4 pool of 1.9 ± 1.3 t CH_4 in near-seafloor waters. These values, particularly the dissolved CH_4 estimation, likely represent lower bounds on actual values. Additionally, the region we mapped only represents a fraction of possible seepage area along the central Chilean Margin, and further exploration is needed to increase spatial coverage of this region and identify any additional methane seeps.

Inclusion in Global Research Statement

This research was conducted as part an oceanographic expedition that was a collaboration between Chilean, American, and European scientists and co-led by Eulogio Soto (Universidad de Valparaíso, Chile), Jeffrey Marlow (Boston University, USA), and Patricia Esquete (Universidade de Aveiro, Portugal). Research and sampling were conducted under Decree 711 No. 13270/760/5 and Research Fishing No. E-224-499, for which we thank the Hydrographic and Oceanographic Service of the Chilean Navy and the Undersecretariat of Fisheries and

Aquaculture, respectively. We additionally thank the customs agents and port staff of Valparaíso and Puerto Montt for their support.

Conflict of Interest

The authors declare no conflicts of interest relevant to this study.

Availability Statement

The bathymetry and watercolumn EM124 data are provided in J. Marlow, 2024a; J. Marlow, 2024b, respectively, and the EM712 data are provided in J. Marlow, 2024c; J. Marlow, 2024d, respectively. Processed multibeam bathymetry data are provided in Beeson et al., 2026. Raw acoustic backscatter and swath bathymetry data from the ROV-mounted M3 system are provided in SOI Data Manager, 2025. Geolocated CH_4 data are provided in Wieman et al., 2026.

Acknowledgments

This work was supported by Schmidt Marine Technology Partners (G-22-63744 to APMM and JK), a Woods Hole Oceanographic Institution Ocean Ventures Fund Grant to STW, and NASA award 80NSSC25K7265 to JJM. The authors would additionally like to thank the Schmidt Ocean Institute, the Captain and crew of R/V *Falkor(too)*, the ROV *SuBastian* team, and the rest of the science party of FKt241011 for the role they played in a productive and successful cruise.

References

Argentino, C., Lee, A., Fallati, L., Sahy, D., Birgel, D., Peckmann, J., et al. (2022). Biogeochemistry and timing of methane-derived carbonate formation at Leirdjupet fault complex, SW Barents Sea. *Frontiers in Earth Science*, *10*, 1029471. https://doi.org/10.3389/feart.2022.1029471

Åström, E. K. L., Carroll, M. L., Ambrose, W. G., Sen, A., Silyakova, A., & Carroll, J. L. (2018). Methane cold seeps as biological oases in the high-Arctic deep sea. *Limnology and Oceanography*, *63*(S1), S209–S231. https://doi.org/10.1002/lno.10732

Beeson, J., Skarke, A., Powell, J., Sanchez, A., & Agarwal, M. (2026). Processed bathymetry data (ASCII XYZ format) of the Chilean Margin (FKt241011, 2024) [Dataset]. *Marine Geoscience Data System (MGDS)*. https://doi.org/10.60521/332729

Boetius, A., & Suess, E. (2004). Hydrate Ridge: A natural laboratory for the study of microbial life fueled by methane from near-surface gas hydrates. *Chemical Geology*, *205*(3–4), 291–310. https://doi.org/10.1016/j.chemgeo.2003.12.034

Carretier, S., Tolorza, V., Regard, V., Aguilar, G., Bermúdez, M. A., Martinod, J., et al. (2018). Review of erosion dynamics along the major N-S climatic gradient in Chile and perspectives. *Geomorphology*, *300*, 45–68. https://doi.org/10.1016/j.geomorph.2017.10.016

Di, P., Feng, D., Tao, J., & Chen, D. (2020). Using time-series videos to quantify methane bubbles flux from natural cold seeps in the South China Sea. *Minerals*, *10*(3), 216. https://doi.org/10.3390/min10030216

Elliott, S., Reagan, M., Moridis, G., & Smith, P. C. (2010). Geochemistry of clathrate-derived methane in Arctic ocean waters. *Geophysical Research Letters*, *37*(12), L12607. https://doi.org/10.1029/2010GL043369

Ezat, M. M., Rasmussen, T. L., & Groeneveld, J. (2014). Persistent intermediate water warming during cold stadials in the southeastern Nordic seas during the past 65 k.y. *Geology*, *42*(8), 663–666. https://doi.org/10.1130/G35579.1

Fu, X., Waite, W. F., & Ruppel, C. D. (2021). Hydrate formation on marine seep bubbles and the implications for water column methane dissolution. *Journal of Geophysical Research: Oceans*, *126*(9), e2021JC017363. https://doi.org/10.1029/2021JC017363

García-Tigreros, F., & Kessler, J. D. (2018). Limited acute influence of aerobic methane oxidation on ocean carbon dioxide and pH in Hudson Canyon, Northern U.S. Atlantic Margin. *Journal of Geophysical Research: Biogeosciences*, *123*(7), 2135–2144. https://doi.org/10.1029/2018JG004384

Garreaud, R. D. (2009). The Andes climate and weather. *Advances in Geosciences*, *22*, 3–11. https://doi.org/10.5194/adgeo-22-3-2009

German, C. R., Ramirez-Llodra, E., Baker, M. C., Tyler, P. A., Baco-Taylor, A., Boetius, A., et al. (2011). Deep-water chemosynthetic ecosystem research during the census of marine life decade and beyond: A proposed deep-ocean road map. *PLoS One*, *6*(8), e23259. https://doi.org/10.1371/journal.pone.0023259

Greinert, J. (2008). Monitoring temporal variability of bubble release at seeps: The hydroacoustic swath system GasQuant. *Journal of Geophysical Research*, *113*(C7), C07048. https://doi.org/10.1029/2007JC004704

Joung, D., Ruppel, C., Southon, J., Weber, T. S., & Kessler, J. D. (2022). Negligible atmospheric release of methane from decomposing hydrates in mid-latitude oceans. *Nature Geoscience*, *15*(11), 885–891. https://doi.org/10.1038/s41561-022-01044-8

Kapit, J., & Michel, A. P. M. (2021). Dissolved gas sensing using an anti-resonant hollow core optical fiber. *Applied Optics*, *60*(33), 10354. https://doi.org/10.1364/AO.439787

Kapit, J., Youngs, S., Pardis, W. A., Padilla, A. M., & Michel, A. P. M. (2024). An underwater methane sensor based on laser spectroscopy in a hollow core optical fiber. *ACS Sensors*, *9*(11), 5896–5905. https://doi.org/10.1021/acssensors.4c01563

Kennett, J. P., Cannariato, K. G., Hendy, I. L., & Behl, R. J. (2000). Carbon isotopic evidence for methane hydrate instability during Quaternary interstadials. *Science*, *288*(5463), 128–133. https://doi.org/10.1126/science.288.5463.128

Klaucke, I., Weinrebe, W., Linke, P., Kläschen, D., & Bialas, J. (2012). Sidescan sonar imagery of widespread fossil and active cold seeps along the central Chilean continental margin. *Geo-Marine Letters*, *32*(5), 489–499. https://doi.org/10.1007/s00367-012-0283-1

Knittel, K., & Boetius, A. (2009). Anaerobic oxidation of methane: Progress with an unknown process. *Annual Review of Microbiology*, *63*(1), 311–334. https://doi.org/10.1146/annurev.micro.61.080706.093130

Lamy, F., Hebbeln, D., & Wefer, G. (1998). Terrigenous sediment supply along the Chilean continental margin: Modern regional patterns of texture and composition. *Geologische Rundschau*, *87*(3), 477–494. https://doi.org/10.1007/s005310050223

Law, C. S., Collins, C., Marriner, A., Bury, S. J., Brown, J. C. S., & Rickard, G. (2024). Dispersion and fate of methane emissions from cold seeps on Hikurangi Margin, New Zealand. *Frontiers in Earth Science*, *12*, 1354388. https://doi.org/10.3389/feart.2024.1354388

Leonte, M., Wang, B., Socolofsky, S. A., Mau, S., Breier, J. A., & Kessler, J. D. (2018). Using carbon isotope fractionation to constrain the extent of methane dissolution into the water column surrounding a natural hydrocarbon gas seep in the northern Gulf of Mexico. *Geochemistry, Geophysics, Geosystems*, *19*(11), 4459–4475. https://doi.org/10.1029/2018GC007705

Locarnini, R. A., Mishonov, A. V., Baranova, O. K., Reagan, J. R., Boyer, T. P., Seidov, D., et al. (2024). World Ocean Atlas 2023, Volume 1: Temperature. In A. Mishonov (Ed.), *NOAA atlas NESDIS 89*. National Oceanographic and Atmospheric Administration.

Luff, R., & Wallmann, K. (2003). Fluid flow, methane fluxes, carbonate precipitation and biogeochemical turnover in gas hydrate-bearing sediments at Hydrate Ridge, Cascadia Margin: Numerical modeling and mass balances. *Geochimica et Cosmochimica Acta*, *67*(18), 3403–3421. https://doi.org/10.1016/S0016-7037(03)00127-3

19448007, 2026, 20, Downloaded from https://agupubs.onlinelibrary.wiley.com/doi/10.1029/2026GL124079 by Cochrane Chile, Wiley Online Library on [12/10/2026]. See the Terms and Conditions (https://onlinelibrary.wiley.com/terms-and-conditions) on Wiley Online Library for rules of use; OA articles are governed by the applicable Creative Commons License

Malinverno, A., Kastner, M., Torres, M. E., & Wortmann, U. G. (2008). Gas hydrate occurrence from pore water chlorinity and downhole logs in a transect across the northern Cascadia margin (Integrated Ocean Drilling Program Expedition 311). *Journal of Geophysical Research*, *113*(B8). https://doi.org/10.1029/2008JB005702

Marcon, Y., Kelley, D., Thornton, B., Manalang, D., & Bohrmann, G. (2021). Variability of natural methane bubble release at Southern Hydrate Ridge. *Geochemistry, Geophysics, Geosystems*, *22*(10), e2021GC009894. https://doi.org/10.1029/2021GC009894

Marlow, J. (2024a). Multibeam sonar (Kongsberg EM124) data as collected during the cruise FKt241011, Canyons, Vents, and Seeps of the Chile Margin [Dataset]. *Rolling Deck to Repository (R2R)*. https://doi.org/10.7284/163379

Marlow, J. (2024b). Multibeam sonar (Kongsberg EM124 [Watercolumn]) data as collected during the cruise FKt241011, Canyons, Vents, and Seeps of the Chile Margin [Dataset]. *Rolling Deck to Repository (R2R)*. https://doi.org/10.7284/163380

Marlow, J. (2024c). Multibeam sonar (Kongsberg EM712) data as collected during the cruise FKt241011, Canyons, Vents, and Seeps of the Chile Margin [Dataset]. *Rolling Deck to Repository (R2R)*. https://doi.org/10.7284/163382

Marlow, J. (2024d). Multibeam sonar (Kongsberg EM712 [watercolumn]) data as collected during the cruise FKt241011, Canyons, Vents, and Seeps of the Chile Margin [Dataset]. *Rolling Deck to Repository (R2R)*. https://doi.org/10.7284/163381

Marlow, J. J., Steele, J. A., Ziebis, W., Thurber, A. R., Levin, L. A., & Orphan, V. J. (2014). Carbonate-hosted methanotrophy represents an unrecognized methane sink in the deep sea. *Nature Communications*, *5*(1), 5094. https://doi.org/10.1038/ncomms6094

Melo, T., Silva, N., Muñoz, P., Díaz-Naveas, J., Sellanes, J., Bravo, A., et al. (2007). Caracterización del fondo marino entre la III y X Regiones. Informe Final Proyecto FIP N°2005-61. Valparaíso, Chile.

Muñoz, P., Cárdenas, L. J., Garbe-Schönberg, D., Sellanes, J., Dezileau, L., Melville, I., & Mendes, S. D. (2016). Geochemical characterization of two distinctive systems with evidence of chemosynthetic activity, explored at the SE Pacific margin off Chile (46°S and 33°S). *Progress in Oceanography*, *148*, 26–43. https://doi.org/10.1016/j.pocean.2016.09.002

Muñoz, P., Castillo, A., Valdés, J., & Dewitte, B. (2023). Oxidative conditions along the continental shelf of the Southeast Pacific during the last two millennia: A multiproxy interpretation of the oxygen minimum zone variability from sedimentary records. *Frontiers in Marine Science*, *10*, 1134164. https://doi.org/10.3389/fmars.2023.1134164

Nordam, T., Dissanayake, A. L., Brakstad, O. G., Hakvåg, S., Øverjordet, I. B., Litzler, E., et al. (2025). Fate of dissolved methane from ocean floor seeps. *Environmental Science and Technology*, *59*(17), 8516–8526. https://doi.org/10.1021/acs.est.5c03297

Padilla, A. M., Pardis, W., Kapit, J., Bjorklund, T. A., Ward, N. D., Fornari, D. J., et al. (2025). Spatial mapping of dissolved methane using an in situ sensor in Puget Sound. *Limnology and Oceanography: Methods*, *23*(11), 804–814. https://doi.org/10.1002/lom3.10717

Panieri, G., Bünz, S., Fornari, D. J., Escartin, J., Serov, P., Jansson, P., et al. (2017). An integrated view of the methane system in the pockmarks at Vestnesa Ridge, 79°N. *Marine Geology*, *390*, 282–300. https://doi.org/10.1016/j.margeo.2017.06.006

Piñero, E., Marquardt, M., Hensen, C., Haeckel, M., & Wallmann, K. (2013). Estimation of the global inventory of methane hydrates in marine sediments using transfer functions. *Biogeosciences*, *10*(2), 959–975. https://doi.org/10.5194/bg-10-959-2013

Preston, V., Flaspohler, G., Kapit, J., Pardis, W., Youngs, S., Martocello, D. E., et al. (2022). Discovering hydrothermalism from Afar: In situ methane instrumentation and change-point detection for decision-making. *Frontiers in Earth Science*, *10*, 984355. https://doi.org/10.3389/feart.2022.984355

Reeburgh, W. S. (2007). Oceanic methane biogeochemistry. *Chemical Reviews*, *107*(2), 486–513. https://doi.org/10.1021/cr050362v

Rehder, G., Leifer, I., Brewer, P. G., Friederich, G., & Peltzer, E. T. (2009). Controls on methane bubble dissolution inside and outside the hydrate stability field from open ocean field experiments and numerical modeling. *Marine Chemistry*, *114*(1–2), 19–30. https://doi.org/10.1016/j.marchem.2009.03.004

Römer, M., Sahling, H., Pape, T., Bohrmann, G., & Spieß, V. (2012). Quantification of gas bubble emissions from submarine hydrocarbon seeps at the Makran continental margin (offshore Pakistan). *Journal of Geophysical Research*, *117*(C10), C10015. https://doi.org/10.1029/2011JC007424

Römer, M., Sahling, H., Pape, T., dos Santos Ferreira, C., Wenzhöfer, F., Boetius, A., & Bohrmann, G. (2014). Methane fluxes and carbonate deposits at a cold seep area of the central Nile Deep Sea Fan, Eastern Mediterranean Sea. *Marine Geology*, *347*, 27–42. https://doi.org/10.1016/j.margeo.2013.10.011

Ruppel, C. D., & Kessler, J. D. (2017). The interaction of climate change and methane hydrates. *Reviews of Geophysics*, *55*(1), 126–168. https://doi.org/10.1002/2016RG000534

Sellanes, J., Quiroga, E., & Gallardo, V. A. (2004). First direct evidence of methane seepage and associated chemosynthetic communities in the bathyal zone off Chile. *Journal of the Marine Biological Association of the United Kingdom*, *84*(5), 1065–1066. https://doi.org/10.1017/S0025315404010422h

Sellanes, J., Quiroga, E., & Neira Sellanes, C. (2008). Megafauna community structure and trophic relationships at the recently discovered Concepción Methane Seep Area, Chile, 36°S. *ICES Journal of Marine Science*, *65*(7), 1102–1111. https://doi.org/10.1093/icesjms/fsn099

SOI Data Manager. (2025). Raw near-bottom ROV acoustic backscatter and swath bathymetry data (M3) acquired during R/V falkor (too) expedition FKt241011 (2024) [Dataset]. *Marine Geoscience Data System (MGDS)*. https://doi.org/10.60521/332266

Suess, E. (2010). Marine cold seeps. In K. N. Timmis (Ed.), *Handbook of hydrocarbon and lipid microbiology* (pp. 185–203). Springer-Verlag Berlin Heidelberg. https://doi.org/10.1007/978-3-540-77587-4_12

Suess, E. (2014). Legacy of hydrate ridge: An illustrated account. In *Proceedings of the 8th international conference on gas hydrates*. Retrieved from https://ir.library.oregonstate.edu/concern/conference_proceedings_or_journals/pk02cc344

Vargas-Cordero, I., Giustiniani, M., Tinivella, U., Villar-Muñoz, L., & Alessandrini, G. (2021). Gas hydrate system offshore Chile. *Energies*, *14*(3), 709. https://doi.org/10.3390/en14030709

Vargas-Cordero, I., Tinivella, U., & Villar-Muñoz, L. (2017). Gas hydrate and free gas concentrations in two sites inside the Chilean Margin (Itata and Valdivia offshores). *Energies*, *10*(12), 2154. https://doi.org/10.3390/en10122154

Vargas-Cordero, I., Tinivella, U., Villar-Muñoz, L., & Bento, J. P. (2018). High gas hydrate and free gas concentrations: An explanation for seeps offshore South Mocha Island. *Energies*, *11*(11), 3062. https://doi.org/10.3390/en11113062

Wallmann, K., Piñero, E., Burwicz, E., Haeckel, M., Hensen, C., Dale, A., & Ruepke, L. (2012). The global inventory of methane hydrate in marine sediments: A theoretical approach. *Energies*, *5*(7), 2449–2498. https://doi.org/10.3390/en5072449

Wang, B., & Socolofsky, S. A. (2015). A deep-sea, high-speed, stereoscopic imaging system for in situ measurement of natural seep bubble and droplet characteristics. *Deep Sea Research Part I: Oceanographic Research Papers*, *104*, 134–148. https://doi.org/10.1016/j.dsr.2015.08.001

Wang, B., Socolofsky, S. A., Breier, J. A., & Seewald, J. S. (2016). Observations of bubbles in natural seep flares at MC 118 and GC 600 using in situ quantitative imaging. *Journal of Geophysical Research: Oceans*, *121*(4), 2203–2230. https://doi.org/10.1002/2015JC011452

Weber, T., Wiseman, N. A., & Kock, A. (2019). Global ocean methane emissions dominated by shallow coastal waters. *Nature Communications*, *10*(1), 4584. https://doi.org/10.1038/s41467-019-12541-7

19448007, 2026, 20, Downloaded from https://agupubs.onlinelibrary.wiley.com/doi/10.1029/2026GL124079 by Cochrane Chile, Wiley Online Library on [12/10/2026]. See the Terms and Conditions (https://onlinelibrary.wiley.com/terms-and-conditions) on Wiley Online Library for rules of use; OA articles are governed by the applicable Creative Commons License

Weldeab, S., Schneider, R. R., Yu, J., & Kylander-Clark, A. (2022). Evidence for massive methane hydrate destabilization during the penultimate interglacial warming. *Proceedings of the National Academy of Sciences of the United States of America*, *119*(35), e2201871119. https://doi.org/10.1073/pnas.2201871119

Wieman, S., Kapit, J., & Michel, A. (2026). Dissolved methane concentrations recorded at cold seeps on the central Chilean Margin [Dataset]. *MBLWHOI Library Dataverse*. https://doi.org/10.26027/DATAWII2ES

Wiesenburg, D. A., & Guinasso, N. L. (1979). Equilibrium solubilities of methane, carbon monoxide, and hydrogen in water and sea water. *Journal of Chemical and Engineering Data*, *24*(4), 2025–2360. https://doi.org/10.1021/je60083a006

Yao, H., Panieri, G., Lehmann, M. F., Himmler, T., & Niemann, H. (2021). Biomarker and isotopic composition of seep carbonates record environmental conditions in two Arctic methane seeps. *Frontiers in Earth Science*, *8*, 570742. https://doi.org/10.3389/feart.2020.570742

Zapata-Hernández, G., Sellanes, J., Thurber, A. R., Levin, L. A., Chazalon, F., & Linke, P. (2014). New insights on the trophic ecology of bathyal communities from the methane seep area off Concepción, Chile (~36° S). *Marine Ecology*, *35*(1), 1–21. https://doi.org/10.1111/maec.12051

References From the Supporting Information

Bayrakci, G., Scalabrin, C., Dupré, S., Leblond, I., Tary, J.-B., Lanteri, N., et al. (2014). Acoustic monitoring of gas emissions from the seafloor. Part II: A case study from the Sea of Marmara. *Marine Geophysical Researches*, *35*(3), 211–229. https://doi.org/10.1007/s11001-014-9227-7

Bright, M., & Lallie, F. (2010). The biology of vestimentiferan tubeworms. *Oceanography and Marine Biology*, *48*, 213–265. https://doi.org/10.1201/ebk1439821169-c4

Holmes, A. M., Oliver, P. G., & Sellanes, J. (2005). A new species of *Lucinoma* (Bivalvia: Lucinoidea) from a methane gas seep off the southwest coast of Chile. *Journal of Conchology*, *38*(6), 673–681. https://doi.org/10.5962/p.408185

Jessen, G. L., Pantoja, S., Gutiérrez, M. A., Quiñones, R. A., González, R. R., Sellanes, J., et al. (2011). Methane in shallow cold seeps at Mocha Island off central Chile. *Continental Shelf Research*, *31*(6), 574–581. https://doi.org/10.1016/j.csr.2010.12.012

Johansen, C., Todd, A. C., & MacDonald, I. R. (2017). Time series video analysis of bubble release processes at natural hydrocarbon seeps in the Northern Gulf of Mexico. *Marine and Petroleum Geology*, *82*, 21–34. https://doi.org/10.1016/j.marpetgeo.2017.01.014

Krylova, E. M., Sellanes, J., Valdés, F., & Delía, G. (2014). *Austrogena*: A new genus of chemosymbiotic bivalves (Bivalvia; Vesicomyidae; Pliocardiinae) from the oxygen minimum zone off central Chile described through morphological and molecular analyses. *Systematics and Biodiversity*, *12*(2), 225–246. https://doi.org/10.1080/14772000.2014.900133

Leifer, I., & Boles, J. (2005). Measurement of marine hydrocarbon seep flow through fractured rock and unconsolidated sediment. *Marine and Petroleum Geology*, *22*(4), 551–568. https://doi.org/10.1016/j.marpetgeo.2004.10.026

Leifer, I., & Culling, D. (2010). Formation of seep bubble plumes in the Coal Oil Point seep field. *Geo-Marine Letters*, *30*(3–4), 339–353. https://doi.org/10.1007/s00367-010-0187-x

Leifer, I., & MacDonald, I. (2003). Dynamics of the gas flux from shallow gas hydrate deposits: Interaction between oily hydrate bubbles and the oceanic environment. *Earth and Planetary Science Letters*, *210*(3–4), 411–424. https://doi.org/10.1016/S0012-821X(03)00173-0

Leifer, I., & Tang, D. (2007). The acoustic signature of marine seep bubbles. *Journal of the Acoustical Society of America*, *121*(1), EL35–EL40. https://doi.org/10.1121/1.2401227

Levin, L. A., Soto, E., Castillo, Y., Esquete, P., & Marlow, J. (2025). Congregation of cusk-eels (*Genypterus chilensis*, Ophidiiformes) at a deep-sea methane seep off Chile. *Ecology*, *106*(10), e70237. https://doi.org/10.1002/ecy.70237

Linke, P. (2011). FS SONNE Fahrtbericht/Cruise Report SO-210 ChiFlux: Identification and investigation of fluid flux, mass wasting and sediments in the forearc of the central Chilean subduction zone, Valparaiso - Valparaiso, 23.09.-01.11.2010. https://doi.org/10.3289/IFM-GEOMAR_Rep_44_2011

Muyakshin, S. I., & Sauter, E. (2010). The hydroacoustic method for the quantification of the gas flux from a submersed bubble plume. *Oceanology*, *50*(6), 995–1001. https://doi.org/10.1134/S0001437010060202

Oliver, P. G., & Sellanes, J. (2005). New species of Thyasiridae from a methane seepage area off Concepción, Chile. *Zootaxa*, *1092*(1092), 1–20. https://doi.org/10.11646/zootaxa.1092.1.1

Quiroga, E., & Sellanes, J. (2009). Two new polychaete species living in the mantle cavity of Calyptogena gallardoi (bivalvia: Vesicomyidae) at a methane seep site off central Chile (~36°S). *Scientia Marina*, *73*(2), 399–407. https://doi.org/10.3989/scimar.2009.73n2399

Sahling, H., Bohrmann, G., Artemov, Y. G., Bahr, A., Brüning, M., Klapp, S. A., et al. (2009). Vodyanitskii mud volcano, Sorokin trough, Black Sea: Geological characterization and quantification of gas bubble streams. *Marine and Petroleum Geology*, *26*(9), 1799–1811. https://doi.org/10.1016/j.marpetgeo.2009.01.010

Sauter, E. J., Muyakshin, S. I., Charlou, J.-L., Schlüter, M., Boetius, A., Jerosch, K., et al. (2006). Methane discharge from a deep-sea submarine mud volcano into the upper water column by gas hydrate-coated methane bubbles. *Earth and Planetary Science Letters*, *243*(3–4), 354–365. https://doi.org/10.1016/j.epsl.2006.01.041

Schneider von Deimling, J., Rehder, G., Greinert, J., McGinnnis, D. F., Boetius, A., & Linke, P. (2011). Quantification of seep-related methane gas emissions at Tommeliten, North Sea. *Continental Shelf Research*, *31*(7–8), 867–878. https://doi.org/10.1016/j.csr.2011.02.012

Sellanes, J., & Krylova, E. (2005). A new species of *Calyptogena* (bivalvia: Vesicomyidae) from a recently discovered methane seepage area off Concepción Bay, Chile (~36°S). *Journal of the Marine Biological Association of the United Kingdom*, *85*(4), 969–976. https://doi.org/10.1017/S0025315405011963

Sellanes, J., Zapata-Hernández, G., Pantoja, S., & Jessen, G. L. (2011). Chemosynthetic trophic support for the benthic community at an intertidal cold seep site at Mocha Island off central Chile. *Estuarine, Coastal and Shelf Science*, *95*(4), 431–439. https://doi.org/10.1016/j.ecss.2011.10.016

Signorelli, J. H., Sellanes, J., & Asorey, C. M. (2021). Bathymodiolinae Mussels in the South-eastern Pacific: The presence of the genus *Adipicola* (Bivalvia: Mytilidae) at a methane seep site off central Chile. *Marine Biology Research*, *17*(5–6), 486–493. https://doi.org/10.1080/17451000.2021.1975754

Stuardo, J., & Valdovinos, C. (1988). A new bathyal *Calyptogena* from off the coast of central Chile (Bivalvia: Vesieomyidae). *Venus*, *47*(4), 241–250.

Turco, F., Ladroit, Y., Watson, S. J., Seabrook, S., Law, C. S., Crutchley, G. J., et al. (2022). Estimates of methane release from gas seeps at the southern Hikurangi Margin, New Zealand. *Frontiers in Earth Science*, *10*, 834047. https://doi.org/10.3389/feart.2022.834047

Veloso, M., Greinert, J., Mienert, J., & De Batist, M. (2015). A new methodology for quantifying bubble flow rates in deep water using splitbeam echosounders: Examples from the Arctic offshore NW-Svalbard. *Limnology and Oceanography: Methods*, *13*(6), 267–287. https://doi.org/10.1002/lom3.10024

19448007, 2026, 20, Downloaded from https://agupubs.onlinelibrary.wiley.com/doi/10.1029/2026GL124079 by Cochrane Chile, Wiley Online Library on [12/10/2026]. See the Terms and Conditions (https://onlinelibrary.wiley.com/terms-and-conditions) on Wiley Online Library for rules of use; OA articles are governed by the applicable Creative Commons License

Veloso-Alarcón, M. E., Urban, P., Weiss, T., Köser, K., She, M., & Greinert, J. (2022). Quantitatively monitoring bubble-flow at a seep site offshore Oregon: Field trials and methodological advances for parallel optical and hydroacoustical measurements. *Frontiers in Earth Science*, *10*, 858992. https://doi.org/10.3389/feart.2022.858992

Wang, B., Jun, I., Socolofsky, S. A., DiMarco, S. F., & Kessler, J. D. (2020). Dynamics of gas bubbles from a submarine hydrocarbon seep within the hydrate stability zone. *Geophysical Research Letters*, *47*(18), e2020GL089256. https://doi.org/10.1029/2020GL089256

19448007, 2026, 20, Downloaded from https://agupubs.onlinelibrary.wiley.com/doi/10.1029/2026GL124079 by Cochrane Chile, Wiley Online Library on [12/10/2026]. See the Terms and Conditions (https://onlinelibrary.wiley.com/terms-and-conditions) on Wiley Online Library for rules of use; OA articles are governed by the applicable Creative Commons License